

Design of Enhanced Wide Band Microstrip Patch Antenna Based on Defected Ground Structures (DGS) for Sub-6 GHz Applications

Mohamed Lemine El Issawi¹,  Dominic Konditi²  and AD Usman³ 

¹Department of Electrical Engineering, Pan African University Institute for Basic Sciences and Technology and Innovation hosted at Jomo Kenyatta University of Agriculture and Technology, Nairobi, Kenya, lemine.mohamed@students.jkuat.ac.ke

²School of Electrical and Electronic Engineering, Faculty of Engineering and Built Environment, Technical University of Kenya (TU-K), Nairobi, Kenya, dominic.konditi@tukenya.ac.ke

³Department of Telecommunication Engineering, Faculty of Engineering, Ahmadu Bello University, Zaria, Nigeria, adusman@abu.edu.ng

*Correspondence: Medlemineelissawi@gmail.com; Tel.: +22247816662

ABSTRACT- In this paper a comprehensive comparative study of three distinct microstrip patch antenna (MPA) designs, each optimized for the sub-6 GHz applications, is presented. The initial design phase utilized a Rogers RT 5880 substrate with a permittivity (ϵ_r) of 2.2 and a thickness (H_1) of 1.42 mm. The proposed model achieved a resonance band ranging from 4.8 to 7 GHz, with a bandwidth of 2.2 GHz and a return loss (S_{11}) of -20 dB. Subsequent enhancements involved integrating a Barium Strontium Titanate (BST) thin film ($\epsilon_r = 250$, thickness (H_2) = 0.005 mm), effectively shifting the operational band to 3.5-5.3 GHz. The final design iteration, which incorporated both BST and a Defective Ground Structure (DGS), represented a substantial advancement, achieving wideband operation from 1.8 to 6 GHz, expanding the bandwidth to 4.2 GHz, and improving the S_{11} to -25 dB. This integration also resulted in a compact antenna size of 30 x 26.5 x 1.42 mm³. These findings underscore the synergistic impact of BST and DGS in enhancing MPA design, marking a significant progression in antenna technology, vital for a range of wireless communication.

Keywords: Microstrip Patch Antenna (MPA), Barium Strontium Titanate (BST), Defected Ground Structures (DGS), Wideband Antenna Design, Sub-6 GHz Applications

ARTICLE INFORMATION

Author(s): Mohamed Lemine El Issawi, Dominic Konditi and AD Usman;

Received: 18/01/24; **Accepted:** 04/03/24; **Published:** 30/03/2024;

E- ISSN: 2347-470X;

Paper Id: IJEER240104;

Citation: 10.37391/IJEER.120143

Webpage-link:

<https://ijeer.forexjournal.co.in/archive/volume-12/ijeer-120143.html>



Publisher's Note: FOREX Publication stays neutral with regard to Jurisdictional claims in Published maps and institutional affiliations.

1. INTRODUCTION

Presently, wireless devices play a pivotal role across various sectors, encompassing telecommunications, aviation, healthcare, and defense. This surge in reliance on wireless technology has necessitated a focused drive by manufacturers towards its enhancement. At the core of these systems lies the antenna, a crucial component responsible for converting electrical impulses into electromagnetic waves for effective transmission and reception [1]. The realm of wireless technology is replete with a diverse spectrum of antenna types, each engineered for specific functional requirements, and their extensive range in applications are well-documented in the scholarly literature of the field. One modern and widely used

antenna type is the microstrip patch antenna (MPA), notable for its relevance in applications demanding compact sizes, such as wearable technology and mobile devices. However, the miniaturization of MPAs poses significant challenges, particularly in maintaining performance efficacy. To address these, researchers have identified three primary methodologies for miniaturizing MPA which include slot integration, shorting and folding techniques, and material loading [2]. The first method (introducing slots) involves decreasing the antenna's size by adding slots or modifying its shape, aiming to maintain substantial electrical length in a smaller area [3–5], in this method, the design parameters of slots and shape can be optimized using genetic algorithms [6–8]. However, this approach often results in complicated geometries and reduced gain. The second method (shorting and folding) for reducing the size of the MPA involves altering the ground plane, typically through the application of Defected Ground Structures (DGS). Researchers have employed various forms of DGS, from simpler configurations like spiral, H-shaped, and U-shaped structures to more intricate designs such as Split-Ring Resonators (SRRs) [9, 10]. While the realization technique of this method offers straightforward implementation, it lacks a uniform design process and often results in antennas with lower efficiency. However, it has the potential to enhance both bandwidth and gain. The third and most straightforward technique for miniaturizing a patch antenna, known as material

loading, involves using a substrate with high relative permittivity (ϵ_r). This approach is based on the principle that the antenna's resonant frequency is inversely proportional to the square root of the product of the substrate's ϵ_r and relative permeability (μ_r). However, a notable limitation of this method is the reduction in bandwidth that typically occurs when employing a substrate with high relative permittivity [11–15].

In recent literature, various approaches to wideband microstrip patch antenna design have been explored, targeting applications of Sub-6 GHz applications. In [16], the study introduced a compact MPA with a $32 \times 32 \times 0.79 \text{ mm}^3$ dimension, employing a Rogers RT 5880 substrate for efficient WiMAX and 5G applications, achieving a -46.78 dB reflection coefficient and 1.40 GHz bandwidth. Another work in [17] designed a Sub-6 GHz wideband antenna on an FR4 substrate, measuring $40 \times 30 \times 1.6 \text{ mm}$, with gains ranging from 1.73 to 3.22 dB . Gokul R et al. developed metamaterial-loaded planar patch antenna, optimized for wideband applications like 5G NR FR1 and Wi-Fi 6E. The antenna uses an FR4 substrate ($\epsilon_r = 4.4$, loss tang 0.025 , and thickness 1.6 mm) and measures $48.6 \text{ mm} \times 52.8 \text{ mm}$. It features Complementary Split Ring Resonator (CSRR) and Square Shaped Cross-Slot (SSCS) in the patch and ground plane, respectively. The design targets enhanced radiation characteristics, focusing on wideband performance in the 5G and Wi-Fi spectrum [18].

A study highlighted the design of a compact, wideband-slotted antenna with DGS, simulated using CADFEKO software. The wide bandwidth was achieved by etching the patch and ground plane of a conventional microstrip antenna. Using an FR4 substrate, the antenna's simplicity and cost-effectiveness were emphasized. Incorporating DGS enhanced its performance, showing a notable frequency shift from 5.5 GHz to 4.84 GHz , which led to a 30% size reduction. This design is suitable for WLAN and satellite uplink applications, meeting standard antenna requirements for miniaturization and bandwidth [19]. Wideband antennas with dual-band characteristics are increasingly preferred in antenna communication systems. A recent study introduced a new design of a MPA exhibiting dual-band functionality. The design reported resonating frequencies at 5.8 GHz and 9.3 GHz , achieving bandwidths of approximately 1100 MHz and 1430 MHz , respectively. It was observed that the 3 dB bandwidth was significantly enhanced after the integration of a DGS and notches into the patch. This antenna effectively covers both S and X bands. The return loss measured for this antenna design was -32.7 dB at 5.8 GHz and -25.03 dB at 9.3 GHz , with the VSWR found to be 1. The CST Microwave Studio software played a pivotal role in the design and simulation processes of the E-Shape patch antenna. The antenna's ability to operate in radar systems at S and X bands, and its simultaneous operation at two distinct bands, was highlighted. These findings provide insights into the performance enhancements achievable with the use of DGS in rectangular microstrip patch antennas [20]. An antenna design simulated using HFSS software, demonstrating operation at resonant frequencies of 2.46 GHz with a DGS and 2.44 GHz without DGS. In this external design, the incorporation of DGS resulted in a 25% increase in bandwidth compared to the non-

DGS variant. However, this modification led to a 19.3% reduction in antenna gain. For the DGS variant, the VSWR was recorded at 1.1359 with a return loss of -23.9298 dB , while the non-DGS version exhibited a VSWR of 1.1347 and a return loss of -24.0024 dB . Additionally, antenna efficiency improved by 2.8% with the implementation of DGS [21]. In a notable study in [22], researchers implemented an L-shaped DGS in a circular microstrip antenna, achieving a remarkable compactness of approximately 91%. This design modification facilitated a shift in the resonant frequency, moving from the second band of WLAN at 5.8 GHz to encompass the GSM band at 1.8 GHz , Bluetooth frequency band at 2.4 GHz , WiMAX band at 3.5 GHz , and the first WLAN band at 5.2 GHz . Further enhancements were made by incorporating dual L-shaped DGS into the ground surface of the antenna, resulting in improved bandwidth characteristics. This development demonstrated both the tunability and bandwidth enhancement capabilities of the proposed circular microstrip antenna design. Research outlined in [23] presents a square microstrip patch antenna, notable for its 7.8% bandwidth. Achieving a broadband response, this design integrates square-shaped cuts in both the radiating patch and ground plane, along with rectangular slots in the radiating patch itself. The antenna's resonant frequency spans from 1.78 GHz to 1.92 GHz , delivering a bandwidth of 138 MHz . A high level of consistency between simulated and measured results substantiates the design's effectiveness.

As technology advances, the need for smaller antennas becomes crucial in order to miniaturize devices, especially in microelectronics. This study presents an innovative MPA design for wideband Sub-6 GHz applications by combining Barium Strontium Titanate (BST) thin films with DGS. This hybrid method greatly decreases antenna size and improves performance, in line with the trend of making wireless communication equipment smaller, representing a substantial progress in antenna technology.

The remaining portion of the manuscript is methodically structured in the following manner: *Section 2* provides a comprehensive explanation of the design approach and procedural aspects. *Section 3* provides a detailed explanation of the findings and comments that were obtained from the study. *Section 4* concludes the paper by summarizing the main results and ideas, and is followed by a list of references.

2. METHOD

This section describes the methodology employed in our research, which focuses on the theoretical modelling and antenna design strategy for the microstrip patch antenna. It is organized into two key subsections to provide a comprehensive and systematic overview of our approach.

2.1 Mathematical Model

In the realm of patch antenna design, the dimensions of a rectangular microstrip antenna are ascertained through empirically derived formulas specific to patch antennas. The length 'L' of the rectangular patch, for instance, is calculated using equation (1).

$$L = L_{eff} - 2\Delta l \quad (1)$$

Length (Effective) is given by:

$$L_{eff} = \frac{c}{2f_r \sqrt{\epsilon_{eff}}} \quad (2)$$

where the effective length, denoted as L_{eff} , and the extension length, represented by Δl , are critical dimensions. The extension length Δl accounts for the gap between the physical and effective lengths of the patch. Equation (3) provides a means to calculate Δl .

$$\Delta l = 0.412h \frac{(\epsilon_{eff}+0.3)\left(\frac{W}{h}+0.264\right)}{(\epsilon_{eff}+0.3)\left(\frac{W}{h}+0.264\right)} \quad (3)$$

In the design of microstrip antennas, several key parameters are crucial for determining the patch dimensions and performance. The dielectric thickness, denoted as h , the patch width, represented by W , and the relative permittivity of the material, ϵ_r , are essential in this calculation process. Equations (4) and (5) in the design methodology specifically address the calculation of the rectangular patch width and the effective dielectric permittivity, respectively.

$$W = \frac{c}{2f_0 \sqrt{\frac{\epsilon_r+1}{2}}} \quad (4)$$

$$\epsilon_{eff} = \frac{\epsilon_r+1}{2} + \frac{\epsilon_r-1}{2} \left(1 + \frac{12h}{W}\right)^{-1} \quad (5)$$

The operating frequency f_r , the speed of light c , the relative permittivity ϵ_r , the thickness h , and the width of the patch W are the parameters depicted in equations (1)-(5) [12].

Equations (6) and equation (7) is used to determine the dimension of the ground plane, there's no need for the calculation of the dimension of the substrate because their dimension is similar.

$$L_g = 6h + L \quad (6)$$

$$W_g = 6h + W \quad (7)$$

The antenna is designed and simulated CST studio (Computer Simulation Technology), is a commercial finite element method solver. The results are expected to show the antenna is able to operate at a frequency range of 1.8 to 6 GHz. antenna fabrication is Rogers RT Duroid 5880, characterized by a thickness(H_1) of 1.42 mm, a low loss tangent of 0.0009, and a relative permittivity constant of 2.2. To achieve wideband the defective ground structure is used.

2.2 Antenna Design

In our study, the antenna's initial structure is presented in figure 1, detailing its foundational geometry. The feeding mechanism, consisting of dimensions $FW \times FL$, is described in table 1. Figure 2 illustrates the second design incorporating BST, with dimensions $G \times GW$ of the partial ground plan as specified in table 1. The final antenna iteration, which includes both BST and DGS, is depicted in figures 3, showcasing the back, and side views respectively, with their dimensions detailed in tables 1 for

the initial design, we used a Rogers RT Duroid 5880 substrate, known for its 1.42 mm thickness (H_1) and low loss tangent of 0.0009. In subsequent designs, we integrated a BST layer with a high permittivity of 250, a thickness (H_2) of 0.005 mm, and a loss tangent of 0.02 as the one used in [24]. The final design's inclusion of DGS, aimed at achieving a wide bandwidth and enhancing antenna performance, is elaborated in figure 3 (a).

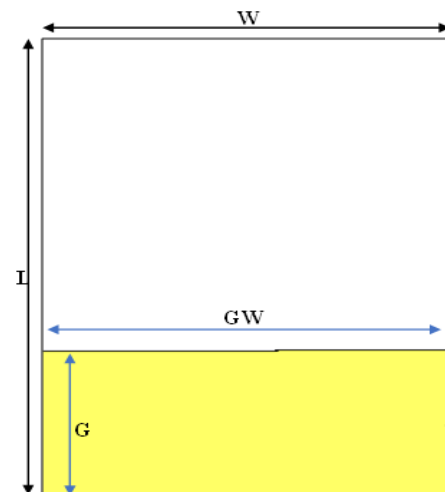
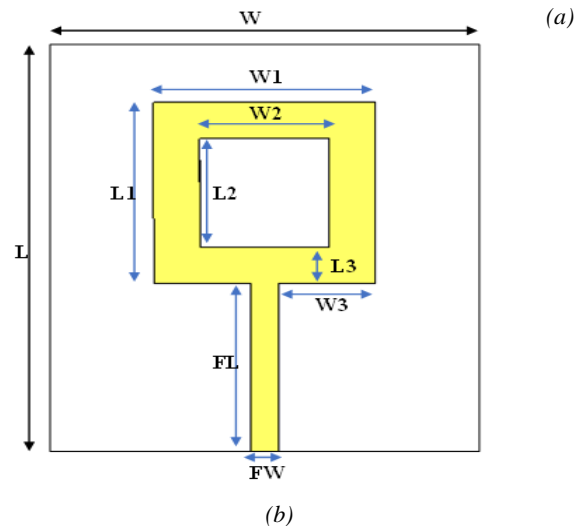
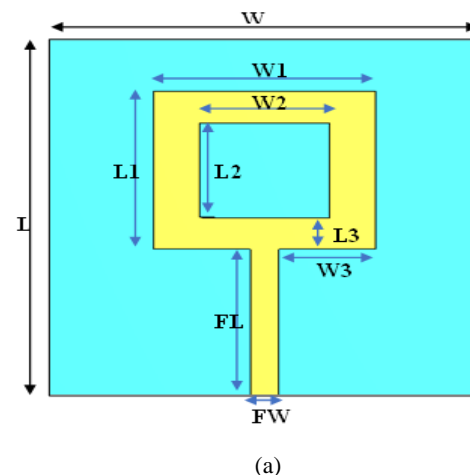


Figure 1: Structure of basic antenna, (a) top view, (b) bottom view



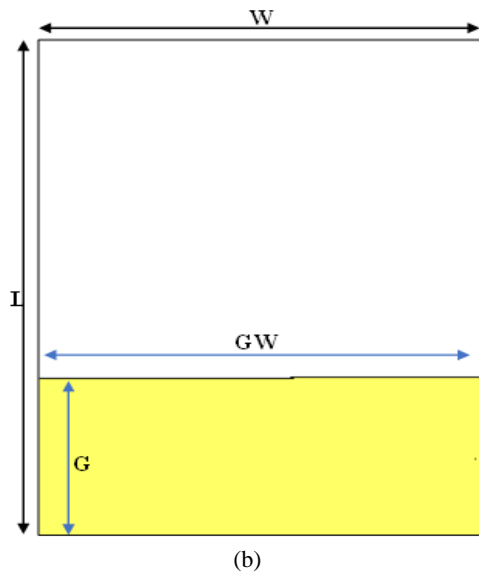


Figure 2: Structure of second antenna with BST Layer, (a) top view, (b) bottom view

Table 1. Antenna design parameters

Parameter	Value (mm)	Parameter	Value (mm)
L	30	L3	3.8
L1	13.2	FW	1.77
L2	7.9	FL	12.3
W	26.5	W3	5.98
W1	13.6	H1	1.42
W2	7.9	H2	0.005
G	9.7	GW	26.5
DGL	20.2	W	26.5
DGL1	3.7	DGL2	5
DGw1	2.7	DGW2	25.8
DGW3	0.7		

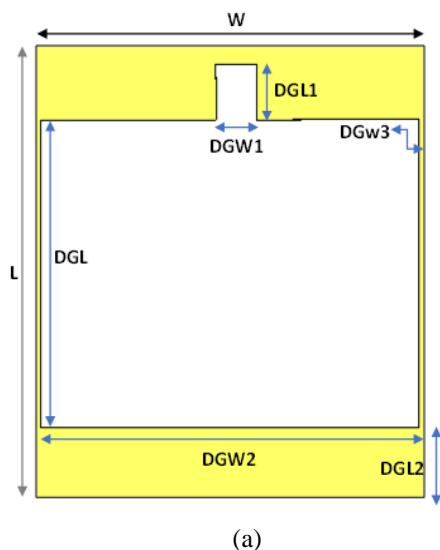


Figure 3: The structure for the final design with BST and DGS, (a) bottom view, (b) side view

3. RESULTS AND DISCUSSIONS

This section presents an in-depth analysis of the results obtained from our study, focusing on the performance metrics of different microstrip patch antenna designs. The evaluations are segmented into three primary cases, each showcasing their respective impacts on key parameters like S parameters and bandwidth.

3.1 S parameters and bandwidth of the antennas

Case 1: Microstrip Patch Antenna without BST

In the initial design, a conventional microstrip patch antenna was utilized, featuring a radiating patch substrate and partial ground. The obtained S_{11} values in *figure 4* indicated resonance within the frequency range of 4.8 to 7 GHz, achieving a peak return loss of -20dB. The resulting bandwidth was measured at 2.2 GHz. This design serves as a baseline for comparison with subsequent configurations.

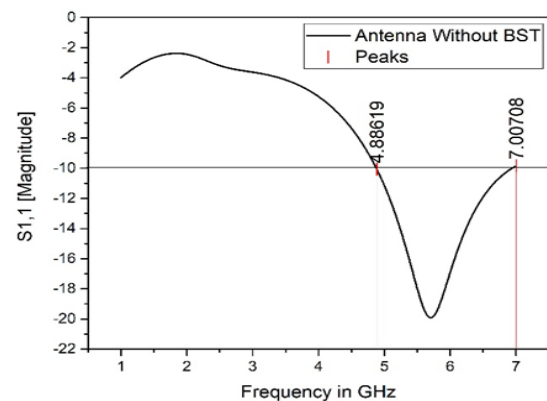


Figure 4: The return loss of antenna without BST

Case 2: Microstrip Patch Antenna with Barium Strontium Titanate (BST)

In the second case, the conventional microstrip patch antenna was augmented with a Barium Strontium Titanate (BST) thin film. This addition led to a shift in the operating bands, resulting in resonance frequencies spanning from 3.5 to 5.4 GHz as showing in *figure 5*. The peak return loss improved to -22dB, and the bandwidth was measured at 1.9 GHz. The incorporation

of BST demonstrates its impact on altering the antenna's characteristics.

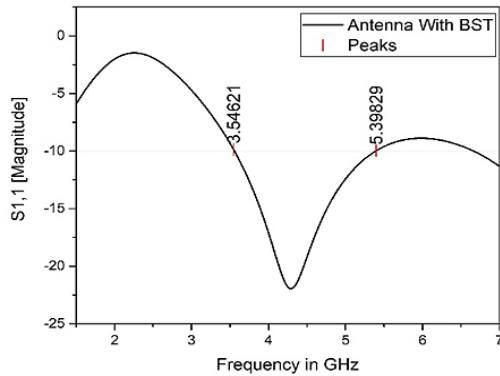


Figure 5: The return loss of antenna with BST

Case 3: Microstrip Patch Antenna with BST and DGS

In the final case, the antenna design was further optimized by integrating both BST and DGS. This comprehensive modification resulted in a notable transformation in performance. The resonance frequencies extended from 1.8 to 6 GHz, achieving a peak return loss of -25dB as shown in figure 6 below. Importantly, the bandwidth was substantially increased to 4.2 GHz, surpassing the achievements of the previous designs. This configuration demonstrates the synergistic effect of combining BST and DGS for enhanced bandwidth in the sub-6 GHz range, covering applications such as WiFi, WLAN, WiMAX, and sub-6 GHz 5G.

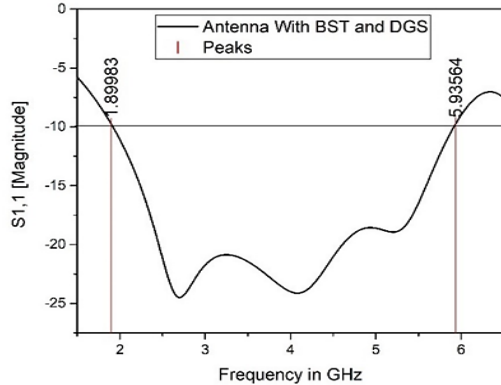


Figure 6: The return loss of antenna with BST and DGS

3.2 Comparison of the three designs

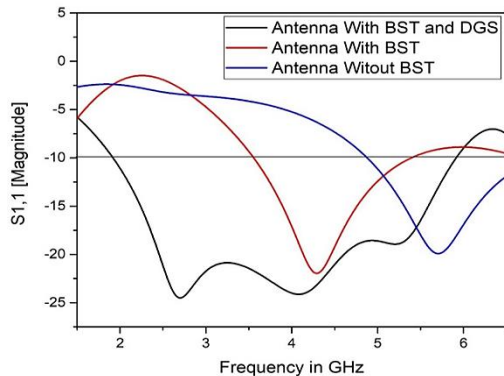


Figure 7: S11 comparison parameters of antenna with BST and DGS

Figure 7 illustrates the reflection coefficient (S11) comparison among three antenna designs: a conventional microstrip patch antenna, an antenna with BST, and an antenna incorporating both BST and DGS. The conventional antenna offers moderate bandwidth at a -20dB level, suitable for specific frequencies. Incorporation of BST enhances the bandwidth, particularly in the lower frequency range, indicating improved suitability for a broader spectrum of applications. The dual enhancement using both BST and DGS achieves the broadest bandwidth, ranging from 1.8 to 6 GHz with a minimum reflection coefficient of -25dB, suggesting its high applicability in sub-6 GHz applications, including WiFi, WLAN, WiMAX, and 5G. The graph underscores the significant bandwidth enhancement achieved by integrating BST and DGS into the antenna design, making it an optimal choice for the specified frequency range and applications.

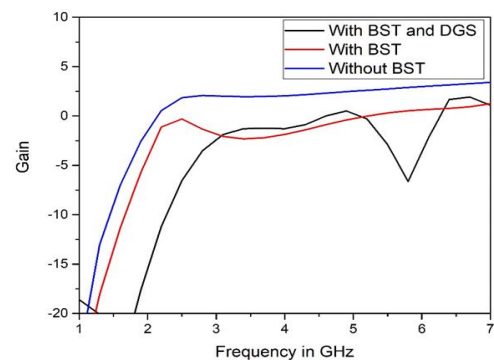


Figure 8: Gain comparison parameters of antenna with BST and DGS

The design process of our microstrip patch antenna began with a conventional configuration without BST, achieving a peak gain of 2.5dBi, indicating strong directionality within the 1 to 7 GHz range. With the integration of BST, the second iteration saw a reduced peak gain of 0.4dBi, suggesting a broader radiation pattern. The final design, which combined BST with DGS, slightly increased the peak gain to 0.5dBi. Despite a modest gain, the significant enhancement in bandwidth due to BST and DGS is evident, which is vital for the antenna's performance in the specified frequency range. This evolution of gain across the design stages is captured in figure 8.

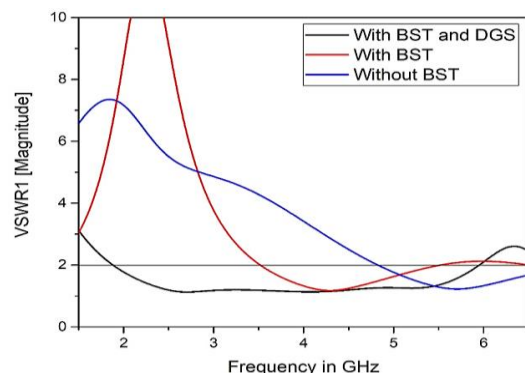


Figure 9: Voltage Standing Wave Ratio (VSWR) comparison

Voltage Standing Wave Ratio is a measure of how efficiently radio-frequency power is transmitted from the source, such as a

transmitter, to the load, such as an antenna. It is expressed as the ratio of the maximum voltage to the minimum voltage along a transmission line. VSWR is a dimensionless quantity, and lower VSWR values indicate better impedance matching.

The VSWR graph for the antenna designs incorporating BST and DGS demonstrates notable impedance matching improvements, as seen in *figure 9*. This enhancement is pivotal for wideband applications, ensuring the antenna maintains effective power transfer across a large frequency range. These results are essential for modern communication systems, highlighting the design's successful adaptation to meet operational standards for WLAN, WiMAX, and sub-6 GHz 5G applications.

Table 2. Comparison of the three designs

S/N	Antenna Design	Frequency (GHz)	S11 (dB)	BW (GHz)
1	Without BST	4.8 to 7	-20	2.2
2	With BST	3.5 to 5.4	-22	1.9
3	With BST and DGS	1.8 to 6	-25	4.2

The results outlined in *table 2* reflect the progressive enhancements made to the antenna design. The initial configuration used a Roger RT 5880 substrate and achieved a resonance within the 4.8 to 7 GHz range, with a 2.2 GHz bandwidth and an S11 of -20 dB. The second design iteration, with the integration of a high-permittivity Barium Strontium Titanate thin film, shifted the resonant frequency to 3.5 to 5.3 GHz. The final design phase incorporated an additional BST layer and a DGS, extending the operational bandwidth to 1.8 to 6 GHz, enhancing the bandwidth to 4.2 GHz, and improving the S11 to -25 dB. This final configuration also achieved a compact form factor with reduction in the antenna's dimensions to 30 x 26.5 x 1.42 mm³, significantly advancing the antenna's design for future wireless applications.

3.3 Comparative analysis

Table 3. Comparative chart of reported work with proposed antenna

Ref.	Size(mm ²)	Frequency (GHz)	Bandwidth (GHZ)	Return loss(dB)
[16]	32x32	3.10-4.50	1.4	-46.78
[17]	40x30	3-5.64	2.64	-27.5
[18]	48.6x52.8	3.09-5.82	2.73	-32.5
[19]	50x40	4.84, 5.96 and 6.34	0.94	-17.2, -18.5, -27.3
[20]	32x40	5.8/ 9.3	1.1/ 1.43	-25.03, -32.7
[21]	55x 60	2.4	0.212	-23.9
[22]	50 x50 mm	1.78 to 1.92	0.138	-33
[23]	34x40	2.4, 3.5 and 5.2	1	-19
This work	30 x 26.5	1.8 to 6	4.2	-25

Table 3 in the manuscript offers a meticulous comparative analysis, juxtaposing the performance of the proposed antenna design with seminal works in the field. The proposed antenna leverages a Defected Ground Structure combined with Barium Strontium Titanate, resulting in a design that is both compact and broad in bandwidth. The empirical evidence suggests that this hybrid integration significantly contributes to the miniaturization and the bandwidth enhancement of the microstrip patch antenna. The data presented underlines the competitive edge of this design, affirming its alignment with and potential superiority over existing research within the domain of antenna technology.

4. CONCLUSION

This research has methodically improved microstrip patch antenna designs for sub-6 GHz frequencies, resulting in a durable and small antenna that integrates BST material and DGS. The initial based on the Roger RT5880 substrate and partial ground plan design yielded a 2 GHz bandwidth and -20 dB S11, which was further enhanced by integration of BST and DGS to a 4.2 GHz bandwidth and -25 dB S11 in the final iteration. The optimization not only increased bandwidth but also reduced the antenna's size significantly. Future work will focus on evaluating alternative materials and the practical realization of the antenna through fabrication and testing, to solidify its application in next-gen wireless communications.

REFERENCES

- [1] A. Reddaff, F. Djerfaff, K. Ferroudji, M. Boudjerda, K. Hamdi-Chérif, and I. Bouchachi, "Design of dual-band antenna using an optimized complementary split ring resonator," *Appl. Phys. A Mater. Sci. Process.*, vol. 125, no. 3, p. 0, 2019, doi: 10.1007/s00339-019-2483-2.
- [2] G. K. Soni, D. Yadav, and A. Kumar, "Design consideration and recent developments in flexible, transparent and wearable antenna technology: A review," *Trans. Emerg. Telecommun. Technol.*, no. July 2023, p. 4894, 2023, doi: 10.1002/ett.4894.
- [3] M. U. Khan, M. S. Sharawi, and R. Mittra, "Microstrip patch antenna miniaturisation techniques: A review," *IET Microwaves, Antennas Propag.*, vol. 9, no. 9, pp. 913–922, 2015, doi: 10.1049/iet-map.2014.0602.
- [4] Z. Chao, Z. Zitong, X. Pei, Y. Jie, L. Zhu, and L. Gaosheng, "A miniaturized microstrip antenna with tunable double band-notched characteristics for UWB applications," *Sci. Rep.*, vol. 12, no. 1, pp. 1–13, 2022, doi: 10.1038/s41598-022-24384-2.
- [5] A. Banerjee, "Planar Spiral Inductors, Planar Antennas and Embedded Planar Transformers," in *Planar Spiral Inductors, Planar Antennas and Embedded Planar Transformers: SPICE-based Design and Performance Evaluation for Wireless Communications*, Springer International Publishing, 2023, pp. 9–88. doi: 10.1007/978-3-031-08778-3.
- [6] J. Venkataraman, A. Wyant, W. Chen, A. Limaye, and G. Shieh, "Small microstrip patch antennas," in *Applied Electromagnetics Conference, AEMC 2009 and URSI Commission B Meeting*, Kolkata, India: IEEE, 2009, pp. 3–6. doi: 10.1109/AEMC.2009.5430662.
- [7] N. Herscovici, M. F. Osorio, and C. Peixeiro, "Miniaturization of rectangular microstrip patches using genetic algorithms," *IEEE Antennas Wirel. Propag. Lett.*, vol. 1, pp. 94–97, 2002, doi: 10.1109/LAWP.2002.805128.
- [8] M. Lamsalli, A. El Hamichi, M. Boussous, N. A. Touhami, and T. E. Elhamadi, "Genetic algorithm optimization for microstrip patch antenna miniaturization," *Prog. Electromagn. Res. Lett.*, vol. 60, no. April, pp. 113–120, 2016, doi: 10.2528/PIERL16041907.
- [9] M. S. Sharawi, M. U. Khan, A. B. Numan, and D. N. Aloï, "A CSRR loaded MIMO antenna system for ISM band operation," *IEEE Trans. Antennas Propag.*, vol. 61, no. 8, pp. 4265–4274, 2013, doi: 10.1109/TAP.2013.2263214.

- [10] J. X. Liu, W. Y. Yin, and S. L. He, "A new defected ground structure and its application for miniaturized switchable antenna," *Prog. Electromagn. Res.*, vol. 107, no. August, pp. 115–128, 2010, doi: 10.2528/PIER10050904.
- [11] N. Altunyurt, M. Swaminathan, P. M. Raj, and V. Nair, "Antenna miniaturization using magneto-dielectric substrates," in *Proceedings - Electronic Components and Technology Conference*, San Diego, CA, USA: IEEE, 2009, pp. 801–808. doi: 10.1109/ECTC.2009.5074103.
- [12] C. A. Balanis, "ANTENNA THEORY ANALYSIS AND DESIGN," in *Encyclopedia of RF and Microwave Engineering*, FOURTH EDI., Canada: John Wiley & Sons, Inc., Hoboken, New Jersey, 2016. doi: 10.1002/0471654507.eme023.
- [13] M. Boudjerda, A. Reddaj, K. Ferrouji, I. Messaoudene, and I. Bouchachi, "Numerical Investigations of a Reconfigurable Patch Antenna using Thin Ferrite Film," 2016. [Online]. Available: <https://api.semanticscholar.org/CorpusID:55556619>
- [14] D. Bonefačić and J. Bartolić, "Small Antennas: Miniaturization Techniques and Applications," *Autom. Control. Meas. Electron. Comput. Commun.*, vol. 53, no. 1, pp. 20–30, 2012, doi: 10.7305/automatika.53-1.164.
- [15] R. Garg, P. Bhartia, I. Bahl, and A. Ittipiboon, *Microstrip Antenna Design Handbook*. 2001.
- [16] L. C. Paul et al., "A Wideband Highly Efficient Omnidirectional Compact Antenna for WiMAX/Lower 5G Communications," *Hindawi, International J. RF Microw. Comput. Eng.*, vol. 2023, p. 10, 2023, doi: 10.1155/2023/7237444.
- [17] P. Jha, S. Singh, R. Yadava, and R. L. Yadava, "Wideband Sub-6 GHz Micro strip Antenna: Design & Fabrication," in *Advances in Smart Communication and Imaging Systems: Select Proceedings of MedCom*, Springer Singapore, 2020, pp. 109–115.
- [18] R. Gokul, D. A. R. T, M. Charan, S. Gnaneshwaran, and G. P. C, "Design of Metamaterial Antenna for Wideband Applications," vol. June, no. June, pp. 8–11, 2023, doi: 10.20944/preprints202306.0630.v1.
- [19] P. K. M. and S. Mohan, "Design of a Triple Band Slit-loaded Patch Antenna with DGS for Bandwidth Enhancement," in *Artificial Intelligence and Evolutionary Algorithms in Engineering Systems: Proceedings of ICAEES 2014*, Springer India, 2015, pp. 823–833. doi: 10.1007/978-81-322-2135-7.
- [20] K. Wagh and S. S. Shriramwar, "Bandwidth Enhancement & Analysis of Microstrip Antenna with DGS for S and X Band Applications," *Int. J. Adv. Sci. Technol.*, vol. 130, pp. 105–114, 2019, doi: 10.33832/ijast.2019.130.10.
- [21] V. R. Anapana, N. Priyanka, and V. P. Sai, "Bandwidth enhancement of a rectangular inset-fed micro-strip patch antenna with DGS for ISM band," in *Proceedings of the 3rd International Conference on Computing Methodologies and Communication, ICCMC 2019*, Erode, India: IEEE, 2019, pp. 638–643. doi: 10.1109/ICCMC.2019.8819843.
- [22] S. Chakraborty et al., "Frequency tuning characteristics & bandwidth enhancement for circular microstrip antenna by integrating I shaped DGS," in *2020 IEEE International IOT, Electronics and Mechatronics Conference (IEMTRONICS)*, IEEE, 2020, pp. 1–7. doi: 10.1109/IEMTRONICS51293.2020.9216423.
- [23] K. D. Girase and M. P. Joshi, "Bandwidth Enhancement of Square Microstrip Patch Antenna Using Defected Ground Structure," in *2018 International Conference On Advances in Communication and Computing Technology, ICACCT 2018*, IEEE, 2018, pp. 325–328. doi: 10.1109/ICACCT.2018.8529575.
- [24] M. Boudjerda et al., "Design and Optimization of Miniaturized Microstrip Patch Antennas Using a Genetic Algorithm," *Electron.*, vol. 11, no. 14, pp. 1–14, 2022, doi: 10.3390/electronics11142123.



© 2024 by Mohamed Lemine El Issawi, Dominic Konditi, AD Usman. Submitted for possible open access publication under the terms and conditions of the Creative Commons Attribution (CC BY) license (<http://creativecommons.org/licenses/by/4.0/>).